Title
Flow-Cytometric Analysis and Purification of Airway Epithelial-Cell Subsets.

Journal
American Journal of Respiratory Cell and Molecular Biology, 64(3)

ISSN
1044-1549

Authors
Bonser, Luke R
Koh, Kyung Duk
Johansson, Kristina
et al.

Publication Date
2021-03-01

DOI
10.1165/rcmb.2020-0149ma

Peer reviewed

Flow-Cytometric Analysis and Purification of Airway Epithelial-Cell Subsets

Luke R. Bonser[1,2], Kyung Duk Koh[1,2], Kristina Johansson[3,4,5], Semil P. Choksi[2], Dan Cheng[1,2,6], Leqian Liu[7], Dingyuan I. Sun[8], Lorna T. Zlock[8], Walter L. Eckalbar[1,9], Walter E. Finkbeiner[8], and David J. Erle[1,2,9]

[1]Lung Biology Center, [2]Cardiovascular Research Institute, [3]Department of Microbiology and Immunology, [4]Division of Pulmonary, Critical Care, Sleep, and Allergy, [5]Sandler Asthma Basic Research Center, [7]Department of Bioengineering and Therapeutic Sciences, [8]Department of Pathology, and [9]University of California, San Francisco CoLabs, University of California San Francisco, San Francisco, California; and [6]Department of Respiratory and Critical Care Medicine, Renmin Hospital, Wuhan University, Wuhan, China

ORCID IDs: 0000-0001-9942-5567 (L.R.B.); 0000-0003-3326-8217 (K.D.K.); 0000-0002-2171-0648 (D.J.E.).

Abstract

The human airway epithelium is essential in homeostasis, and epithelial dysfunction contributes to chronic airway disease. Development of flow-cytometric methods to characterize subsets of airway epithelial cells will enable further dissection of airway epithelial biology. Leveraging single-cell RNA-sequencing data in combination with known cell type–specific markers, we developed panels of antibodies to characterize and isolate the major airway epithelial subsets (basal, ciliated, and secretory cells) from human bronchial epithelial-cell cultures. We also identified molecularly distinct subpopulations of secretory cells and demonstrated cell subset–specific expression of low-abundance transcripts and microRNAs that are challenging to analyze with current single-cell RNA-sequencing methods. These new tools will be valuable for analyzing and separating airway epithelial subsets and interrogating airway epithelial biology.

Keywords: airway epithelium; single-cell RNA sequencing; flow cytometry

Clinical Relevance

We leveraged single-cell RNA-sequencing data sets to develop flow-cytometric panels to characterize and isolate the major airway epithelial subsets (basal, ciliated, and secretory cells) from human bronchial epithelial-cell cultures. These panels identified major airway epithelial-cell subsets, revealed molecular heterogeneity within these populations, and permitted analysis of low-abundance transcripts and microRNAs. We envisage that these panels and their future refinements will be powerful tools for interrogating airway epithelial biology in human health and disease.

Flow cytometry is a commonly used research and diagnostic tool that uses fluorophore-conjugated antibodies as probes to identify, characterize, and/or isolate cell populations (1). The immunology community has developed panels of antibodies useful for detailed immunophenotyping of immune cells derived from many organs, including the lung. A recent American Thoracic Society working-group report (2) heralded the importance of flow cytometry in pulmonary research but noted that "the development of appropriate markers for nonimmunologic cells is less mature than other pulmonary cell types," including epithelial cells.

(Received in original form April 20, 2020; accepted in final form November 16, 2020)

Supported by U.S. National Institutes of Health grants U19 AI 077439, R35 HL145235, and R01 HL138424 (D.J.E.); National Institutes of Health grant DK072517 and Cystic Fibrosis Foundation Grant DR613-CR11 (W.E.F.); and a University of California, San Francisco, Program for Breakthrough Biomedical Research Postdoctoral Independent Research Project Award (L.R.B.).

Author Contributions: L.R.B. and D.J.E. contributed to the study conception and design. L.R.B. developed the novel experimental methods. L.R.B., K.D.K., K.J., S.P.C., D.C., L.L., D.I.S., and L.T.Z. performed the experiments. L.R.B., K.D.K., K.J., D.C., L.L., W.L.E., and D.J.E. analyzed data. L.R.B. and D.J.E. interpreted data. W.E.F. and D.J.E. supervised the study execution. L.R.B., K.D.K., and D.J.E. drafted the manuscript. All authors revised the manuscript.

Correspondence and requests for reprints should be addressed to David J. Erle, M.D., University of California, San Francisco, Cardiovascular Research Institute Mail Code: 3118, 555 Mission Bay Boulevard South, Post Office Box 589001, San Francisco, CA 94158-9001. E-mail: david.erle@ucsf.edu.

This article has a data supplement, which is accessible from this issue's table of contents at www.atsjournals.org.

Am J Respir Cell Mol Biol Vol 64, Iss 3, pp 308–317, Mar 2021

Originally Published in Press as DOI: 10.1165/rcmb.2020-0149MA on November 16, 2020
Internet address: www.atsjournals.org

The airway epithelium defends against inhaled environmental challenges, including pollutants, pathogens, and allergens (3), and epithelial dysfunction is central to the pathogenesis of major lung diseases, including asthma, cystic fibrosis, chronic obstructive pulmonary disease, and primary ciliary dyskinesia (4). Proximal airway epithelial subsets, including basal cells, ciliated cells, secretory cells (including club and goblet cells), intermediate cells, brush cells, and pulmonary neuroendocrine cells, have been defined morphologically and by their anatomical location within the tissue using histological analysis and EM (5, 6). Single-cell RNA-sequencing (scRNA-seq) is further advancing our understanding of airway epithelial heterogeneity. Recent studies of human and murine airways have confirmed the presence of previously defined major airway epithelial subsets, identified molecularly distinct subpopulations of these cells, and uncovered previously unrecognized cell types, including ionocytes (7–11).

Pan-epithelial antibodies (EpCAM/pan-cytokeratin) (12) and limited sets of cell type–specific antibodies (e.g., TUBA [acetylated α tubulin] for ciliated cells [13], NGFR [nerve growth factor receptor] and ITGA6 [integrin subunit α 6] [14] for basal cells, and MUC5AC for goblet cells [15]) have been used individually for flow cytometry. We sought to develop a larger panel of antibodies for simultaneous analysis of the major subsets of airway epithelial cells and provide a new tool for further understanding airway epithelial physiology and pathology. To this end, we used known markers described elsewhere in the literature, augmented these by leveraging information from scRNA-seq datasets, and developed panels of antibodies for flow cytometry to identify, characterize, and isolate the major human-airway epithelial subsets.

Some of the results of these studies have been previously reported in the form of abstract (16) and in the form of a preprint (https://doi.org/10.1101/2020.04.20.051383).

Methods

Additional methodological details are provided in the data supplement. A detailed step-by-step protocol is also provided as a Supplementary Document.

Primary Human Bronchial Epithelial-Cell Culture

Human bronchial epithelial cells (HBECs) isolated from explanted tissue from lung-transplant donor recipients or from lungs not used for transplantation (total $n = 12$; *see* Table E1 in the data supplement) were cultured at air–liquid interface (ALI) as previously described (17, 18). We harvested cells 23 days after establishment of ALI. Some cultures were stimulated with IL-13 (10 ng/ml; PeproTech, Inc.) for the final seven days of culture to induce goblet-cell production as indicated (19). The University of California, San Francisco, Committee on Human Research approved the use of HBECs for these studies.

Flow-Cytometric Analysis

We trypsinized HBECs to generate single-cell suspensions and fixed cells in 0.5% (vol/vol) paraformaldehyde; if not stained immediately, cells were frozen at −80°C. Cells were blocked, stained with the analytical panel (Table 1), and analyzed by flow cytometry.

Flow-Cytometric Cell Sorting

Before trypsinization, cells were incubated in culture media containing SiR-Tubulin (Cytoskeleton, Inc.). Single-cell suspensions were generated as above, and singlets were stained with fixable viability dye eFluor450 (Thermo Fisher Scientific) to discriminate live cells. Cells were subsequently stained with a sorting panel (Table 1) and isolated using flow cytometric cell sorting.

Gene Expression Analysis

We isolated total RNA from sorted cells, performed reverse transcription, and analyzed cDNA by qRT-PCR to quantify specific mRNAs and microRNAs (miRNAs). Table E2 lists qRT-PCR primer sequences.

Results

Identification of Airway Epithelial-Subset Markers

To identify a panel of candidate cell subset–specific markers, we combined markers previously used for flow cytometry (TUBA [ciliated], ITGA6 and NGFR [basal], and MUC5AC [goblet]) with transcripts identified in several recent human scRNA-seq data sets (CDHR3 [cadherin-related family member 3; ciliated] and CEACAM5 [carcinoembryonic antigen-related cell-adhesion molecule 5; secretory]) (7, 9–11). We also analyzed HBECs differentiated at ALI (17, 18) using the Drop-seq scRNA-seq platform (20); IL-13–stimulated cultures were included, as IL-13 induces goblet-cell production (19) (Figure E1A). We examined our data set for cell type–specific transcripts (Figure E1B), defined as genes more highly expressed in one cell type than the others (false discovery rate < 0.05) and identified two additional markers CEACAM6 (secretory) and TSPAN8 (tetraspanin-8; goblet). We combined all markers into a prospective flow panel (Table 2). CD24, which has previously been used as a ciliated-cell marker for flow cytometry (21), was also tested but was omitted from the panel because of a complex staining pattern (*see* data supplement).

To test whether these putative cell-subset markers were suitable for flow cytometry, we stained unstimulated and IL-13–stimulated HBECs from five individuals with antibodies against these markers individually and performed flow cytometry. Each antibody stained a subset of HBECs from both unstimulated and IL-13–stimulated cell cultures, except for the goblet-cell markers TSPAN8 and MUC5AC, which stained a subset of cells from IL-13–stimulated cultures but stained few if any cells from unstimulated cultures (Figure 1A). We observed significant increases in cells staining for TSPAN8 ($P = 0.022$) and MUC5AC ($P = 0.0016$) after IL-13 stimulation; however, we did not observe statistically significant effects of IL-13 stimulation on the proportion of cells stained for the other markers (Figure 1B).

Characterization of Airway Epithelial-Cell Subsets Using an Analytical Antibody Panel

To assess whether we could combine the cell-subset markers to identify major airway epithelial subsets, we stained unstimulated and IL-13–stimulated HBECs from five individuals with an analytical panel comprising all eight antibodies (Table 1) and performed multicolor flow cytometry. We used a sequential gating strategy to identify major airway epithelial subsets (Figures 2A–2E and E2); positive staining

Table 1. Antibody Details

Stain/Antigen	Gene	Fluorophore	Clone	Isotype	Source	Catalog Number	Concentration ($\mu g/ml$)	Ab/test (μl)	Ab/test (μg)	Location	Target Cell
Analytical panel											
TUBA	TUBA1A, etc.*	AF647	6-11B-1	mIgG2b	Santa Cruz Biotechnology, Inc.	sc-23950	200	1	0.2	IC	Ciliated
CDHR3	*CDHR3*	R-PE	HPA011218	rpAb	MilliporeSigma	HPA011218	100	1	0.1	CSM	Ciliated
CD49f	*ITGA6*	PE-CF594	GoH3	ratIgG2a	BD	562493	NA	0.25	NA	CSM	Basal
CD271	*NGFR*	PE Cy7	ME20.4	mIgG1	BioLegend	345110	100	0.1	0.01	CSM	Basal
CD66c	*CEACAM6*	BV510	B6.2	mIgG1	BD	742684	200	1	0.2	CSM	Secretory
CD66e	*CEACAM5*	APC	487609	mIgG2a	R&D Systems	MAB41281	NA	1	NA	CSM	Secretory
TSPAN8	*TSPAN8*	AF405	458811	ratIgG2b	R&D Systems	FAB4734V	200	1.5	0.3	CSM	Goblet
MUC5AC	*MUC5AC*	APC Cy7	45M1	mIgG1	Thermo Fisher Scientific	MS-145-PABX	1,000	0.25	0.25	IC	Goblet
Sorting panel											
SiR-tubulin	*TUB1A1*, etc.	674	NA	NA	Cytoskeleton, Inc.	CY-SC002	50	0.05	NA	IC	Ciliated
Fixable viability dye	NA	eFluor450	NA	NA	Invitrogen	65-0863-18	NA	0.5	NA	NA	Live cells
CD271	*NGFR*	PE Cy7	ME20.4	mIgG1	Biolegend	345110	100	0.1	0.01	CSM	Basal
CD66c	*CEACAM6*	BV510	B6.2	mIgG1	BD	742684	200	1	0.2	CSM	Secretory
TSPAN8	*TSPAN8*	FITC	FAB4734V	ratIgG2b	R&D Systems	FAB4734V	200	0.5	0.1	CSM	Goblet

Definition of abbreviations: Ab = antibody; AF647/405 = Alexa Fluor 647/405; APC = allophycocyanin; BD = Becton Dickinson and Company; BV510 = Brilliant Violet 510; CDHR3 = cadherin-related family member 3; *CEACAM* = CEA cell-adhesion molecule 5; CSM = cell surface (membrane); Cy7 = cyanine7; FITC = fluorescein isothiocyanate; IC = intracellular; *ITGA6* = integrin subunit α 6; mIgG1 = mouse immunoglobulin G, Fcγ subclass 1; mIgG2a = mouse immunoglobulin G, Fcγ subclass 2a; mIgG2b = mouse immunoglobulin G, Fcγ subclass 2b; NA = information not available/provided by manufacturer *NGFR* = nerve growth factor receptor; ratIgG2a = rat immunoglobulin G, Fcγ subclass 2a; ratIgG2b = rat immunoglobulin G, Fcγ subclass 2b. rpAb = rabbit polyclonal antibody; R-PE = R-Phycoerythrin; TSPAN8 = tetraspanin-8; TUBA = acetylated α-tubulin.
*This antibody recognizes acetylated forms of multiple TUBA family members.

Table 2. Panel of Cell Subset–Specific Markers

Name	Antigen	Cell Subset	Description	References
Acetylated α-tubulin	TUBA	Ciliated	Recognizes axonemal α-tubulin acetylated on the epsilon-amino group of lysine(s), a hallmark of stable microtubules, which are enriched in motile cilia	7, 9, 10, 23, 32
Cadherin-related family member 3	CDHR3	Ciliated	Calcium-dependent cell-adhesion protein associated with ciliogenesis and asthma; receptor for rhinovirus C	9, 10, 13, 33, 34
Integrin subunit α 6	CD49f/ITGA6	Basal	Integral membrane protein of the integrin α chain family; function uncharacterized in the airway	10, 14
Nerve growth factor receptor	CD271/NGFR	Basal	Cell-surface receptor localized to basal cells of unknown function in the airway	7, 14
CEA cell-adhesion molecule 5	CD66c/CEACAM5	Secretory	Cell-surface glycoprotein upregulated after smoking cessation and linked to lung squamous-cell carcinoma	9, 10, 35, 36
CEA cell-adhesion molecule 6	CD66e/CEACAM6	Secretory	Cell-surface glycoprotein associated with severe asthma and upregulated after smoking cessation	7, 9, 10, 35, 37
Tetraspanin 8	TSPAN8	Goblet	Cell-surface glycoprotein of unknown function in the airway	9, 10
MUC5AC	MUC5AC	Goblet	Secreted, gel-forming glycoprotein associated with mucus dysfunction in chronic lung disease	4, 9, 10

was determined using either fluorescence-minus-one or matched isotype controls (*see* data supplement, Figure E3). Cells staining for the ciliated-cell marker TUBA were clearly distinct from those staining for the basal-cell marker NGFR. $TUBA^-NGFR^-$ cells could be further classified on the basis of staining with other markers: a minority expressed the basal-cell marker ITGA6, whereas many expressed the secretory-cell marker CEACAM6. Within the $CEACAM6^+$ secretory-cell population, staining for the goblet-cell marker MUC5AC was largely confined to the $TSPAN8^+$ population that emerged after IL-13 stimulation. CDHR3 and CEACAM5 were not used as part of this standard sequential gating strategy (additional details are presented in the data supplement).

We quantified the proportion of four major epithelial-cell subsets in five donors (Figure 2F). Because results from three donors with interstitial lung disease were similar to those from the remaining two donors with no history of airway or lung disease, we combined all five donors to analyze the effects of IL-13 on epithelial-cell subsets. HBECs derived from individuals with no history of airway disease ($n = 2$) had similar proportions of ciliated ($TUBA^+NGFR^-$), basal ($TUBA^-NGFR^+$ and $TUBA^-NGFR^-CEACAM6^-ITGA6^+$), and secretory cells ($TUBA^-NGFR^-CEACAM6^+ITGA6^-$) as those derived from individuals with interstitial lung disease ($n = 3$). IL-13 stimulation resulted in a consistent increase in the proportion of secretory cells ($TUBA^-NGFR^-CEACAM6^+ITGA6^-$; $P = 0.0079$ by Wilcoxon signed-rank test) and goblet cells ($TUBA^-NGFR^-CEACAM6^+ITGA6^-TSPAN8^+MUC5AC^+$; $P = 0.0075$), and a trend toward a decrease in the proportion of ciliated cells in response to IL-13 ($P = 0.056$). To assess the reproducibility of flow-cytometric quantification, we cultured cells from three frozen aliquots originating from two individuals with no history of airway disease on separate occasions and analyzed the cells by using flow cytometry. Cell-type proportions were highly consistent among replicates (Figure E4), indicating that the culture and flow-cytometric methods give reproducible results, even when replicates are conducted on separate occasions. Variation among replicates was modest compared with variation among samples from different donors. Variation among samples from different donors may represent interindividual differences or differences in the harvesting or processing of the samples before cell culture.

The standard gating strategy was useful for quantifying major subsets but did not fully represent the complexity of the airway epithelium, as revealed by staining with the full eight marker panel. When considering all 2^8 (256) possible marker-staining combinations, we identified 12 subsets comprising at least 1% of total cells in unstimulated cultures. After IL-13 stimulation, 17 such subsets were identified, 6 were unique to IL-13–stimulated cultures and were accounted for by an increase in the number of cells bearing secretory-cell markers (CEACAM6, CEACAM5, TSPAN8, and MUC5AC); among these IL-13–induced subsets were also cells costaining for ciliated- and secretory-cell markers (*see* data supplement and Table E3).

To explore heterogeneity further, we analyzed the 10-dimensional data set (one fluorescence intensity for each of the eight antibodies, forward scatter, and side scatter) using *t*-distributed stochastic neighbor embedding (Figures 2G–2R). The distribution of marker staining indicated that cell-type heterogeneity was the major driver of staining patterns in this data set, although IL-13 stimulation (Figure 2Q) and interdonor variation (Figure 2R) also contributed to the staining patterns. We next examined each staining parameter in relation to the *t*-distributed stochastic neighbor embedding plot. TUBA staining (Figure 2G) was confined to a distinct cluster of cells that were predominantly $CDHR3^+$ (Figure 2H); cells bearing these two ciliated-cell markers had little if any basal cell– or secretory cell–marker staining. Another cluster comprised cells stained for the basal-cell markers NGFR (Figure 2I) and ITGA6 (Figure 2J), but with little if any secretory cell– or ciliated cell–marker staining, except for a small

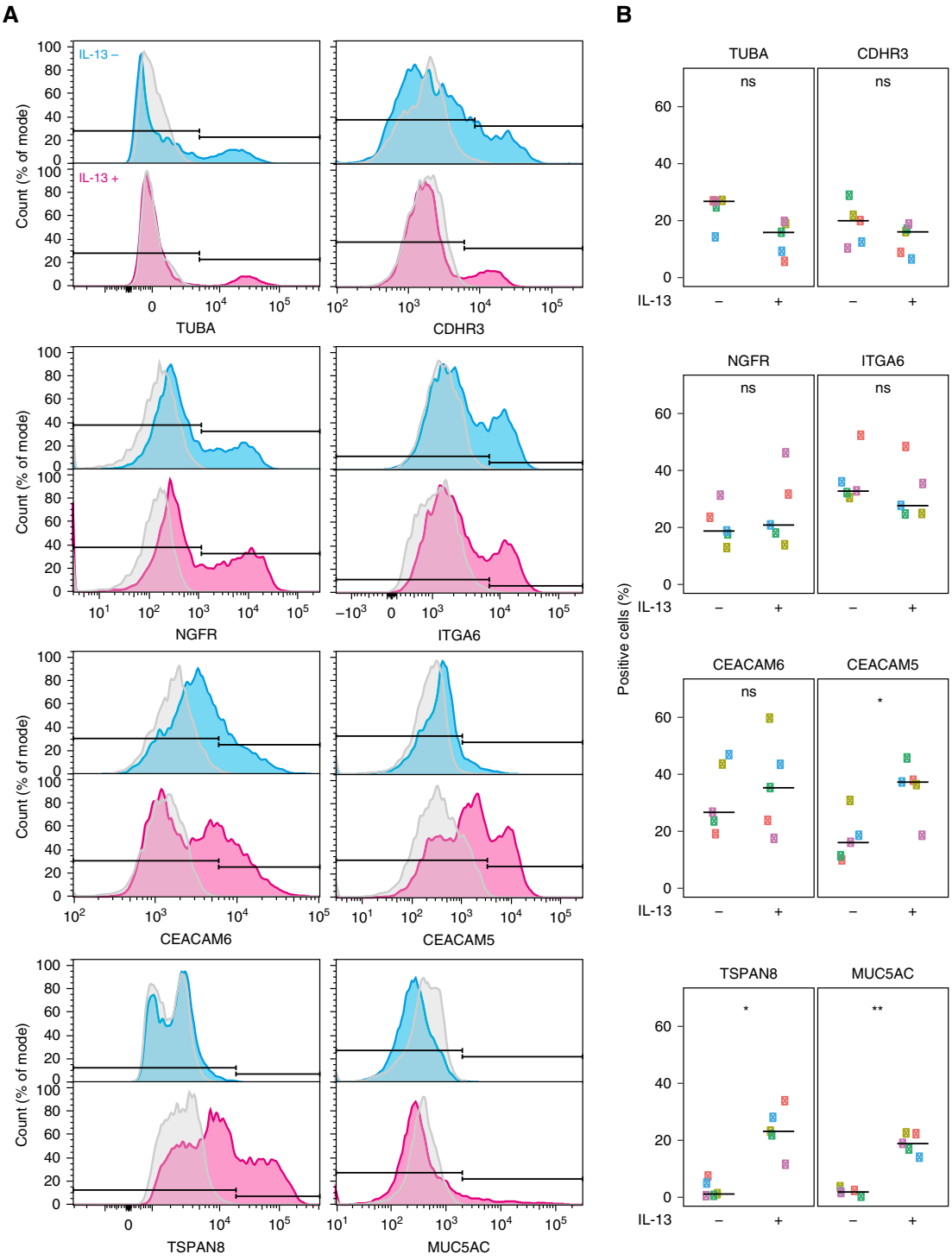

Figure 1. Identification of cell-specific markers for flow cytometry. (*A*) Human bronchial epithelial cells (HBECs) grown in the absence (cyan histogram) or presence of IL-13 (magenta histogram) were stained using antibodies against cell subset–specific markers. Positive staining was determined by comparing the same sample stained with an appropriate isotype control (gray histogram). Histograms represent data from a single experiment with one donor; data from 10,000 cells were acquired. (*B*) Comparison of positive staining for cell subset–specific markers from unstimulated and IL-13–stimulated HBECs (staining of one technical replicate from $n = 5$ individuals; each donor is represented by a different color). Significance was evaluated using a Wilcoxon signed-rank test: $^{*}P < 0.05$ and $^{**}P < 0.01$. CDHR3 = cadherin-related family member 3; CEACAM = carcinoembryonic antigen-related cell-adhesion molecule 5; ITGA6 = integrin subunit α 6; NGFR = nerve growth factor receptor; ns = nonsignificant; TSPAN8 = tetraspanin-8; TUBA = acetylated α-tubulin.

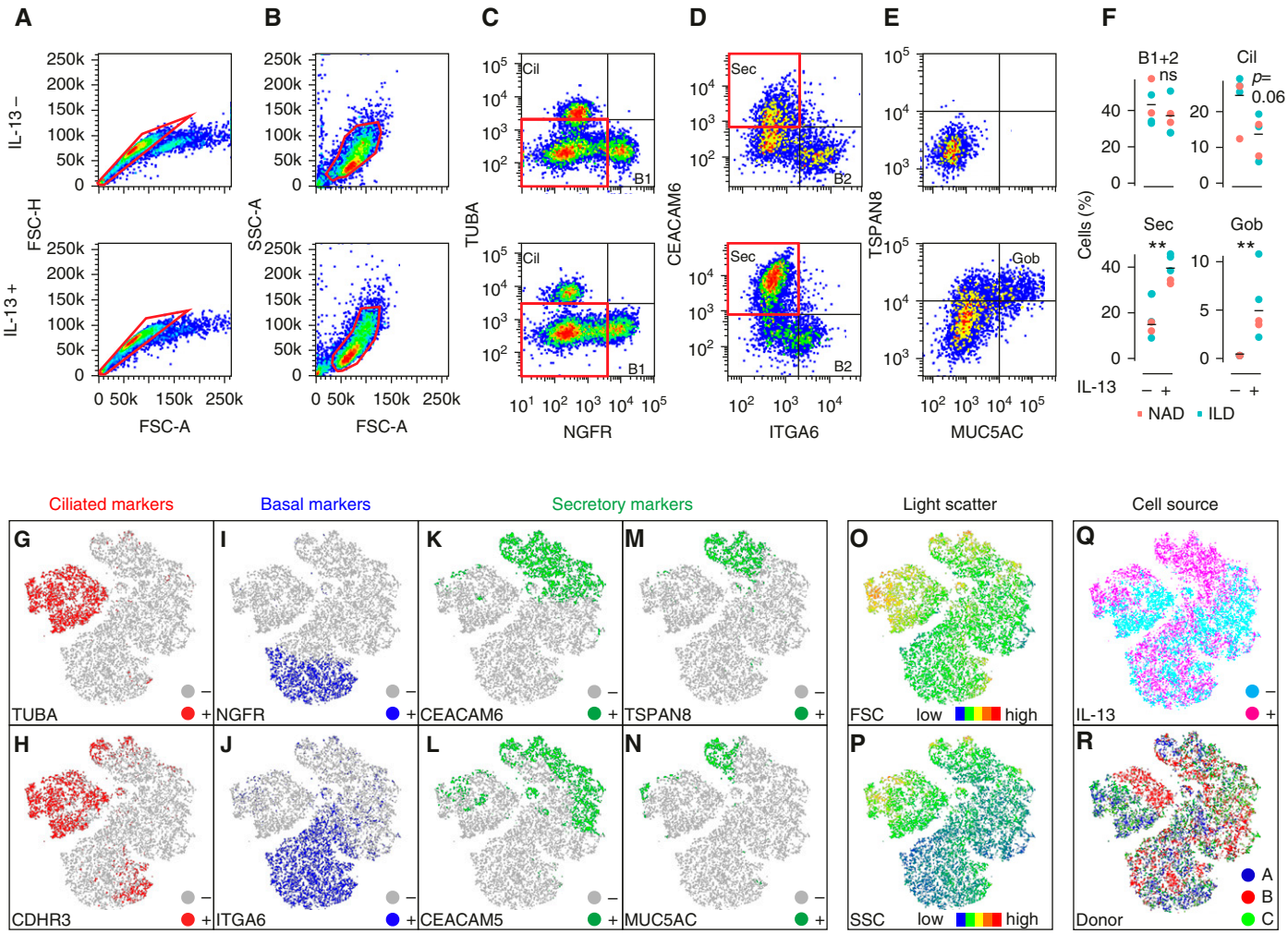

Figure 2. Characterization of airway epithelial-cell subsets and IL-13 stimulation using an analytical flow-cytometric panel. HBECs ($n = 5$ donors) were cultured with or without IL-13 and processed for multicolor flow cytometry. Data from 10,000 cells originating from a single replicate were acquired. (*A–E*) Gating strategy to identify airway epithelial subsets from unstimulated (IL-13$^-$) and IL-13–stimulated (IL-13$^+$) HBECs. (*A*) Doublets and (*B*) debris were removed, and resulting singlets were gated on (*C*) NGFR and TUBA. (*D*) Subsequently, TUBA$^-$NGFR$^-$ singlets were gated on ITGA6 and CEACAM6. (*E*) ITGA6$^-$CEACAM6$^+$ cells were then gated on MUC5AC and TSPAN8. The specific gate used in the subsequent analysis step is outlined in red. Positive antibody staining was determined using fluorescence-minus-one controls. Although antibodies for CDHR3 and CEACAM5 were also included in the panel, they were not used in our standard gating method because of substantial overlap with TUBA and CEACAM6 staining, respectively. (*F*) Quantification of four major epithelial subsets (B1+2; ciliated [Cil], TUBA$^+$NGFR$^-$; secretory [Sec], TUBA$^-$NGFR$^-$CEACAM6$^+$ITGA6$^-$; and Gob, TUBA$^-$NGFR$^-$CEACAM6$^+$ITGA6$^-$TSPAN8$^+$MUC5AC$^+$) from unstimulated (IL-13$^-$) and IL-13–stimulated (IL-13$^+$) HBECs derived from two individuals with no history of airway disease (NAD, pink) and three individuals with interstitial lung disease (ILD, cyan). The black bar represents the mean across HBECs, irrespective of disease history. (*G–R*) After downsampling, flow-cytometric results from 3,000 cells from each of three donors were combined and analyzed by *t*-distributed stochastic neighbor embedding. The *t*-distributed stochastic neighbor embedding plots are colored to show cells that stained for the ciliated cell markers (*G*) TUBA and (*H*) CDHR3 (red), the basal-cell markers (*I*) NGFR and (*J*) ITGA6 (blue), and the secretory cell markers (*K*) CEACAM6, (*L*) CEACAM5, (*M*) TSPAN8, and (*N*) MUC5AC (green). Cells that did not stain for the indicated marker are shown in gray. (*O*) FSC and (*P*) SSC are represented as a continuum from low (blue) to high (red). Cells came from unstimulated ($^-$; cyan) or IL-13–stimulated ($^+$; pink) (*Q*) cultures from three (*R*) individuals (*R*) (the *R* should be after individual rather than three; similarly (*Q*) could be moved after cultures 3 words earlier) (donors A, B, and C). $^{**}P < 0.01$ for unstimulated versus IL-13–stimulated by Wilcoxon rank-sum test. B1 = TUBA$^-$NGFR$^+$; B2 = TUBA$^-$NGFR$^-$CEACAM6$^-$ITGA6$^+$; B1+2 = sum of B1 and B2; FSC = forward scatter; Gob = goblet; ILD = interstitial lung disease; NAD = no history of airway disease; ns = not significant; SSC = side scatter.

subset that stained for CDHR3. Cells that stained for neither ciliated- nor basal-cell markers generally stained with antibodies against one or both of the secretory-cell markers CEACAM5 (Figure 2K) and CEACAM6 (Figure 2L). CEACAM5 staining was more pronounced in IL-13–stimulated cells. TSPAN8 and MUC5AC were detected only after IL-13 stimulation. TSPAN8 staining was limited to a subset of CEACAM5$^+$ cells (Figure 2M); MUC5AC staining was

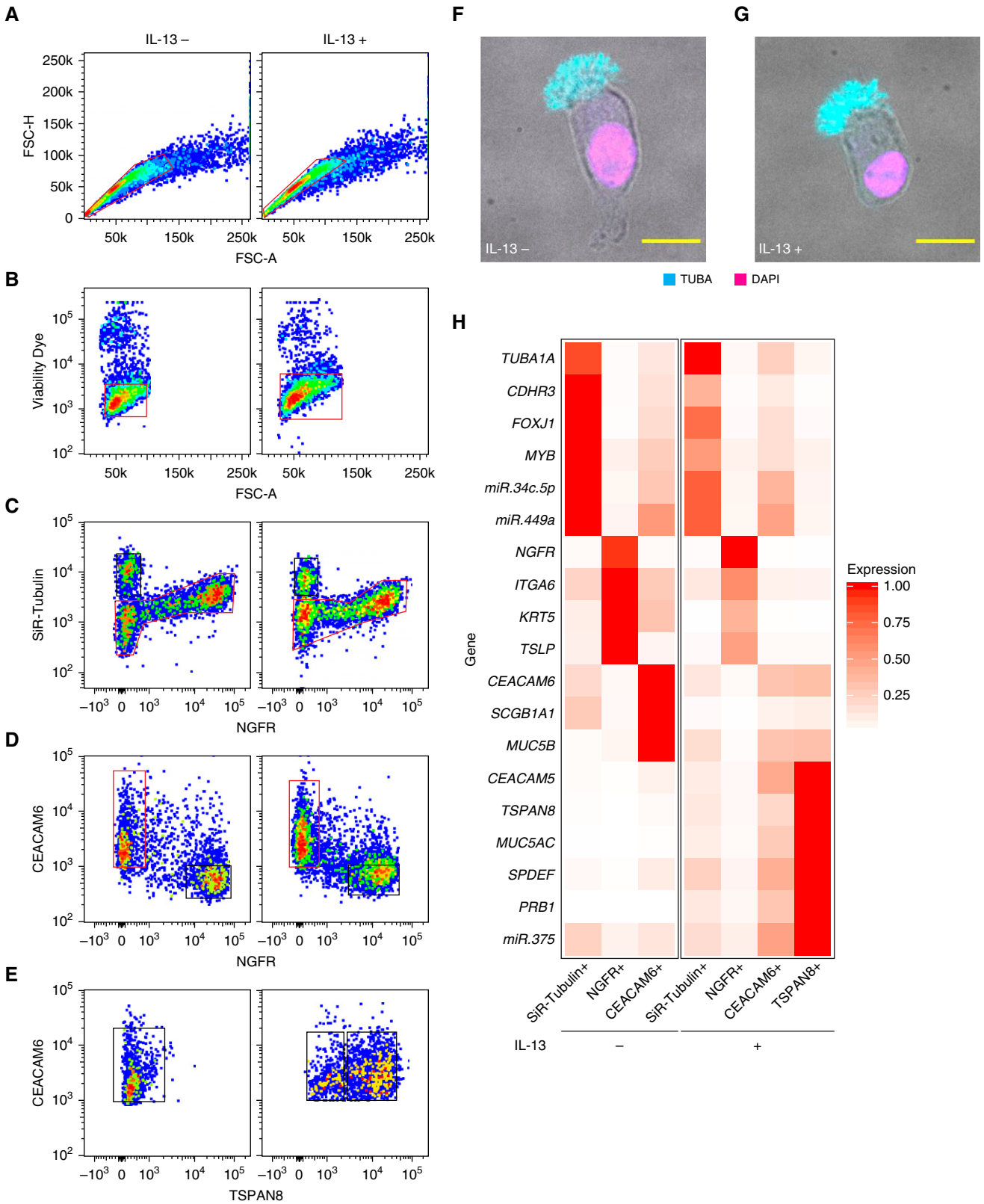

Figure 3. Flow-cytometric sorting of HBEC subsets. Before processing for flow cytometry, six 12-mm Transwells each of HBECs ($n = 3$ donors) cultured in the absence or presence of IL-13 were stained with SiR-tubulin. SiR-tubulin–stained cells were trypsinized, stained with a cell-viability dye, and sorted by flow cytometric cell sorting. (*A–E*) Gating strategy for flow-cytometric cell sorting of unstimulated (IL-13$^-$) and IL-13–stimulated (IL-13$^+$) HBECs for

evident in a subset of the TSPAN8$^+$ population (Figure 2N). Ciliated cells (TUBA$^+$ and CDHR3$^+$) and some secretory cells tended to have higher forward scatter (Figure 2O), an indicator of cell size, and basal cells (ITGA6$^+$ and frequently NGFR$^+$) tended to have lower side scatter (Figure 2P). Further work will be required to determine the functional significance of the many subpopulations identified using this panel.

To explore whether antibodies from our panel might be useful for analyses of cells obtained directly from human airways, we analyzed freshly isolated cells obtained from endobronchial brush biopsy by using immunofluorescence (Figure E5). Ciliated cells were readily recognized by the numerous apical cilia and costained for TUBA and CDHR3; staining for markers of other subsets was not evident in cells bearing cilia. NGFR$^+$ cells were smaller and had a high nuclear-to-cytoplasmic ratio, as expected for basal cells. CEACAM6-stained cells often contained MUC5B-stained granules, consistent with expression in secretory cells. TSPAN8-stained cells frequently contained collections of larger, MUC5AC-stained granules characteristic of goblet cells. Staining for ciliated- and basal-cell markers was not observed in cells replete with cytoplasmic granules. These data indicate that our panel may also be useful for characterizing airway epithelial subsets in clinical samples, although further work will be required to optimize flow cytometry for use with endobronchial brush biopsy specimens or other human tissue samples.

A Modified Flow-Cytometric Panel is Suitable for Live-Cell Sorting

Flow cytometry is also useful for live-cell sorting. Our analytical panel precludes this because it requires fixation and permeabilization for staining with antibodies against the intracellular antigens MUC5AC and TUBA. We therefore designed a sorting panel that omitted the MUC5AC antibody and replaced the TUBA antibody with SiR-tubulin, a membrane-permeable live-cell dye that stains microtubules (22), which have a major structural role in cilia (23). To recover live cells and improve RNA integrity, we also included a viability dye. The sorting panel is detailed in Table 1.

To evaluate this panel, we performed flow-cytometric cell sorting on nonfixed HBECs from three donors (Figures 3A–3E). After excluding dead cells that failed to exclude the viability dye, we gated on SiR-tubulin and NGFR and identified the SiR-tubulin$^+$NGFR$^-$ singlets. Sorted SiR-tubulin$^+$NGFR$^-$ cells were subsequently stained for TUBA and examined by microscopy; 58 of 60 cells examined possessed cilia and stained with TUBA, confirming that these were ciliated cells (Figures 3F and 3G). We gated the remaining singlets on CEACAM6 and NGFR staining to discriminate between secretory- and basal-cell subpopulations. NGFR$^-$CEACAM6$^+$ cells were then gated on CEACAM6 and TSPAN8 staining to identify goblet cells.

We subsequently sorted these HBEC subsets. Purity was assessed by flow-cytometric analysis of sorted cells (Figure E6), and yield was assessed by counting sorted cells (Table E4). Subsequently, we isolated total RNA and performed qRT-PCR for cell type–specific markers (Figure 3H). As expected, the ciliated-cell transcripts *FOXJ1* (forkhead box J1), *TUBA1A* (tubulin α 1A), and *CDHR3* were enriched in the SiR-tubulin$^+$ ciliated-cell subset; expression of these transcripts was reduced by IL-13 stimulation, suggesting that IL-13 affects the transcriptional program of ciliated cells. The basal-cell transcripts *KRT5* (cytokeratin 5) and *NGFR* were enriched in the NGFR$^+$ basal-cell subset; this subset also expressed *ITGA6*. The secretory-cell transcripts, *SCGB1A* (secretoglobulin family 1A member 1; also known as *CCSP* [club cell–specific protein) and *MUC5B*, together with *CEACAM6*, were enriched in the CEACAM6$^+$ secretory-cell subset, as expected. The goblet-cell transcripts *SPDEF* (SAM pointed domain–containing ETS transcription factor), *MUC5AC*, and *TSPAN8* were upregulated in CEACAM6$^+$TSPAN8$^+$ cells from IL-13–stimulated HBEC cultures. Collectively, this analysis demonstrated that the combination of cell-surface-marker and SiR-tubulin staining was sufficient for discriminating the major airway epithelial-cell populations.

Analyzing sorted cells may improve the ability to detect low-abundance transcripts that are difficult to quantify using available scRNA-seq approaches. We identified several transcripts detected in a bulk RNA-seq data set (24) but absent from our scRNA-seq data set and performed qRT-PCR to determine their cell subset–specific expression. For example, the transcription factor *SPDEF* is critical for IL-13–induced goblet-cell differentiation of HBECs (15) but was not detected in our scRNA-seq data set. Using our sorting panel, we found that *SPDEF* was selectively expressed in CEACAM6$^+$ secretory cells, particularly CEACAM6$^+$TSPAN8$^+$ cells (Figure 3D). The alarmin *TSLP* (thymic stromal lymphopoietin) was almost exclusively expressed in the NGFR$^+$ basal-cell subset. The ciliated-cell transcription factor *MYB* (MYB protooncogene, transcription factor) (25) was expressed primarily in SiR-tubulin$^+$ ciliated cells and was downregulated by IL-13. Expression of the secreted protein, *PRB1* (proline-rich protein BstNI subfamily 1), which we identified as an IL-13–induced gene by bulk RNA-seq but did not detect using Drop-seq, was enriched

Figure 3. (*Continued*). a representative donor. After selection of (*A*) singlets and (*B*) live cells, cells were gated on (*C*) SiR-tubulin and NGFR staining. (*D*) SiR-tubulin$^-$ cells were gated on NGFR and CEACAM6. (*E*) NGFR$^-$CEACAM6$^+$ cells were gated on CEACAM6 and TSPAN8. The specific gate/quadrant used in the subsequent analysis step is outlined in red. (*F* and *G*) To validate SiR-tubulin staining, SiR-tubulin$^+$ cells were fixed in paraformaldehyde, immobilized to slides by cytospin, stained with TUBA (cyan), and counterstained with DAPI (magenta). Images show a representative cell from (*F*) unstimulated (IL-13$^-$) and (*G*) IL-13–stimulated (IL-13$^+$) cultures with TUBA-stained cilia (found in 58/60 cells examined). Scale bars, 10 μM. (*H*) qRT-PCR analysis of sorted cell subpopulations. Mean expression values calculated from triplicate experiments with different donors ($n = 3$) were normalized to the maximum expression of the gene in any cell type (0–1: white to red). *CFTR* = cystic fibrosis transmembrane conductance regulator; *DCLK1* = doublecortin-like kinase 1; *FOXJ1* = forkhead box J1; *KRT5* = cytokeratin 5; miR = microRNA; *MYB* = MYB proto-oncogene, transcription factor; *PRB1* = proline-rich protein BstNI subfamily 1; *SCGB1A* = secretoglobulin family 1A member; *SPDEF* = SAM pointed domain–containing ETS transcription factor; *TSLP* = thymic stromal lymphopoietin; *TUBA1A* = tubulin α 1A class 1.

in the CEACAM6$^+$TSPAN8$^+$ secretory-cell subset.

Analyzing sorted cells also allows for analysis of small RNAs, such as miRNAs, that are not assessed using Drop-seq and related scRNA-seq approaches. miR-34/449 family miRNAs are required for motile ciliogenesis (26). We quantified miR-34c-5p and miR-449a and confirmed enrichment in SiR-tubulin$^+$ ciliated cells. We found that miR-375, which is involved in goblet-cell differentiation in the colon (27), was IL-13 inducible, restricted to secretory cells, and enriched in the TSPAN8$^+$ secretory-cell subset. These data demonstrate that the sorting strategy we developed is useful for isolating and characterizing subpopulations of epithelial cells with distinct transcriptional and miRNA profiles.

Discussion

Our study outlines an analytical flow panel and gating strategy for the characterization and enumeration of subsets of airway epithelial cells from HBECs. We also demonstrate a scheme for isolating common airway epithelial subsets from HBECs using a sorting flow panel. Both panels identified major airway epithelial subsets—ciliated cells, basal cells, and secretory cells—as well as molecularly distinct subsets of each.

Our data underline the increasing recognition of airway epithelial-cell heterogeneity and illustrate the value of combining several markers in flow-cytometric panels. Cell-type diversity was increased in response to IL-13, largely accounted for by changes in secretory-cell subsets, including the emergence of TSPAN8$^+$ and MUC5AC$^+$ subsets. Increases in MUC5AC production are important in asthma pathogenesis (19). Tetraspanins are transmembrane proteins that play roles in cell signaling, and the observation that MUC5AC was detected largely in TSPAN8$^+$ cells suggests a possible role for this tetraspanin in regulating mucus production and/or secretion in asthma. The detection of MUC5AC in some cells that express both secretory-cell markers (CEACAM5 and/or CEAMCAM6) together with ciliated-cell markers (CDHR3 and/or TUBA) suggests additional complexity and may relate to previous work showing that goblet cells can be produced from ciliated-cell progenitors (28).

In total, our data suggest that airway epithelial subsets may be more precisely described by sets of molecular markers than by using traditional approaches for defining ciliated, basal, and secretory cells on the basis of morphology and/or use of more limited sets of markers (29). Traditionally, nomenclature is based principally on histological criteria (5, 6) that fail to capture the heterogeneity evident from scRNA-seq (7–11) or antibody panels. Our protocol provides a working method for classifying airway epithelial subsets, and we expect that additional reagents can be added to this panel to further subdivide major subsets and identify other smaller populations, such as ionocytes. Furthermore, use of standard sets of molecular markers such as those developed here will promote clearer communication and allow for more meaningful comparisons across studies.

We coupled flow-cytometric cell sorting with gene expression analysis and identified mRNA transcripts not detected in our scRNA-seq experiment plus several miRNAs. Although scRNA-seq is revealing airway epithelial-cell transcriptomes in unprecedented resolution, current technologies have limited sensitivity and do not reliably detect low-abundance transcripts (e.g., transcription factors) that may have significant impact on cell specification and in disease. Furthermore, available scRNA-seq techniques are generally not suited for analyzing mRNA variants or small RNAs, such as miRNAs. Therefore, our sorting panel may contribute to deeper cataloging of airway epithelial-subset transcriptomes. In addition, our panels could be coupled with downstream epigenetic and proteomic analyses to further understand the specification and/or function of airway epithelial subsets in human health and disease.

There is potential to build on the protocols we have developed. For example, although flow-cytometric analysis of clinical samples was not performed, we demonstrate staining of airway epithelial cells isolated by endobronchial brushing, and published scRNA-seq data sets suggest that the panels we developed could be useful for analyzing disaggregated cells from human airways (7, 9–11). Furthermore, although our study used a 10-parameter, 8-fluorochrome approach, future refinement and the addition of other markers for rarer epithelial subtypes (e.g., *CFTR* [cystic fibrosis transmembrane conductance regulator]–expressing ionocytes and *DCLK1* [doublecortin-like kinase 1]–expressing tuft cells) (7–10) may permit characterization of the null or minor (<1%) populations reported here. A limitation of our study is that in some cases, we studied samples from a limited number of donors, many of whom had interstitial lung disease. Hence, larger studies including more healthy control subjects and well-characterized subjects with disease will be important for understanding normal heterogeneity and how this changes in disease. In addition, combining the epithelial panel with existing panels for immune cells and other nonepithelial cells will permit a more comprehensive examination of lung development, airway inflammation, and immune responses across the hematopoietic and epithelial compartments. Mass cytometry (30) or use of oligonucleotide-barcoded antibodies together with single-cell sequencing (31) also promise to allow for more extensive panels of markers that could further expand our approach to increase our understanding of the function of specific subsets and their heterogeneity.

In summary, we have leveraged scRNA-seq data sets to develop flow-cytometric panels for characterizing subpopulations of airway epithelial cells. These panels identified major airway epithelial-cell subsets, revealed molecular heterogeneity within these populations, and permitted analysis of low-abundance transcripts and miRNAs. We envisage that these panels and their future refinements will be powerful tools for interrogating airway epithelial biology. ■

Author disclosures are available with the text of this article at www.atsjournals.org.

Acknowledgment: The authors thank Paul Wolters for providing lung tissue and donor information and Joshua Pollack for his help analyzing Drop-seq data. We also thank the University of California, San Francisco, Nikon Imaging Center and Laboratory for Cell Analysis for advice and assistance with microscopy and flow cytometry, respectively.

References

1. Maecker HT, McCoy JP, Nussenblatt R. Standardizing immunophenotyping for the Human Immunology Project. *Nat Rev Immunol* 2012;12:191–200.
2. Tighe RM, Redente EF, Yu Y-R, Herold S, Sperling AI, Curtis JL, *et al*. Improving the quality and reproducibility of flow cytometry in the lung: an official American Thoracic Society workshop report. *Am J Respir Cell Mol Biol* 2019;61:150–161.
3. Bonser LR, Erle DJ. The airway epithelium in asthma. *Adv Immunol* 2019;142:1–34.
4. Bonser LR, Erle DJ. Airway mucus and asthma: the role of MUC5AC and MUC5B. *J Clin Med* 2017;6:112.
5. Rhodin J. LXVII ultrastructure of the tracheal ciliated mucosa in rat and man. *Ann Otol Rhinol Laryngol* 1959;68:964–974.
6. Widdicombe JH. Early studies on the surface epithelium of mammalian airways. *Am J Physiol Lung Cell Mol Physiol* 2019;317:L486–L495.
7. Plasschaert LW, Žilionis R, Choo-Wing R, Savova V, Knehr J, Roma G, *et al*. A single-cell atlas of the airway epithelium reveals the CFTR-rich pulmonary ionocyte. *Nature* 2018;560:377–381.
8. Montoro DT, Haber AL, Biton M, Vinarsky V, Lin B, Birket SE, *et al*. A revised airway epithelial hierarchy includes CFTR-expressing ionocytes. *Nature* 2018;560:319–324.
9. Ordovas-Montanes J, Dwyer DF, Nyquist SK, Buchheit KM, Vukovic M, Deb C, *et al*. Allergic inflammatory memory in human respiratory epithelial progenitor cells. *Nature* 2018;560:649–654.
10. Duclos GE, Teixeira VH, Autissier P, Gesthalter YB, Reinders-Luinge MA, Terrano R, *et al*. Characterizing smoking-induced transcriptional heterogeneity in the human bronchial epithelium at single-cell resolution. *Sci Adv* 2019;5:eaaw3413.
11. Ruiz García S, Deprez M, Lebrigand K, Cavard A, Paquet A, Arguel M-J, *et al*. Novel dynamics of human mucociliary differentiation revealed by single-cell RNA sequencing of nasal epithelial cultures. *Development* 2019;146:dev177428.
12. Maestre-Batlle D, Pena OM, Hirota JA, Gunawan E, Rider CF, Sutherland D, *et al*. Novel flow cytometry approach to identify bronchial epithelial cells from healthy human airways. *Sci Rep* 2017;7:42214.
13. Griggs TF, Bochkov YA, Basnet S, Pasic TR, Brockman-Schneider RA, Palmenberg AC, *et al*. Rhinovirus C targets ciliated airway epithelial cells. *Respir Res* 2017;18:84.
14. Rock JR, Onaitis MW, Rawlins EL, Lu Y, Clark CP, Xue Y, *et al*. Basal cells as stem cells of the mouse trachea and human airway epithelium. *Proc Natl Acad Sci USA* 2009;106:12771–12775.
15. Koh KD, Siddiqui S, Cheng D, Bonser LR, Sun DI, Zlock LT, *et al*. Efficient RNP-directed human gene targeting reveals SPDEF is required for IL-13-induced mucostasis. *Am J Respir Cell Mol Biol* 2020;62:373–381.
16. Bonser L, Eckalbar W, Koh KD, Zlock L, Bolourchi S, Joo A, *et al*. Cell type-specific epigenomic and transcriptomic responses to asthma-associated cytokines [abstract]. *Am J Respir Crit Care Med* 2019;199: A3806.
17. Fulcher ML, Gabriel S, Burns KA, Yankaskas JR, Randell SH. Well-differentiated human airway epithelial cell cultures. In: Picot J, editor. Human cell culture protocols, Totowa, NJ: Humana Press; 2005. pp. 183–206.
18. Whitcutt MJ, Adler KB, Wu R. A biphasic chamber system for maintaining polarity of differentiation of cultured respiratory tract epithelial cells. *In Vitro Cell Dev Biol* 1988;24:420–428.
19. Bonser LR, Zlock L, Finkbeiner W, Erle DJ. Epithelial tethering of MUC5AC-rich mucus impairs mucociliary transport in asthma. *J Clin Invest* 2016;126:2367–2371.
20. Macosko EZ, Basu A, Satija R, Nemesh J, Shekhar K, Goldman M, *et al*. Highly parallel genome-wide expression profiling of individual cells using nanoliter droplets. *Cell* 2015;161:1202–1214.
21. Chen H, Matsumoto K, Brockway BL, Rackley CR, Liang J, Lee J-H, *et al*. Airway epithelial progenitors are region specific and show differential responses to bleomycin-induced lung injury. *Stem Cells* 2012;30:1948–1960.
22. Lukinavičius G, Reymond L, D'Este E, Masharina A, Göttfert F, Ta H, *et al*. Fluorogenic probes for live-cell imaging of the cytoskeleton. *Nat Methods* 2014;11:731–733.
23. Oltean A, Schaffer AJ, Bayly PV, Brody SL. Quantifying ciliary dynamics during assembly reveals stepwise waveform maturation in airway cells. *Am J Respir Cell Mol Biol* 2018;59:511–522.
24. Christenson SA, van den Berge M, Faiz A, Inkamp K, Bhakta N, Bonser LR, *et al*. An airway epithelial IL-17A response signature identifies a steroid-unresponsive COPD patient subgroup. *J Clin Invest* 2019; 129:169–181.
25. Pan JH, Adair-Kirk TL, Patel AC, Huang T, Yozamp NS, Xu J, *et al*. Myb permits multilineage airway epithelial cell differentiation. *Stem Cells* 2014;32:3245–3256.
26. Song R, Walentek P, Sponer N, Klimke A, Lee JS, Dixon G, *et al*. miR-34/449 miRNAs are required for motile ciliogenesis by repressing cp110. *Nature* 2014;510:115–120.
27. Biton M, Levin A, Slyper M, Alkalay I, Horwitz E, Mor H, *et al*. Epithelial microRNAs regulate gut mucosal immunity via epithelium-T cell crosstalk. *Nat Immunol* 2011;12:239–246.
28. Turner J, Roger J, Fitau J, Combe D, Giddings J, Heeke GV, *et al*. Goblet cells are derived from a FOXJ1-expressing progenitor in a human airway epithelium. *Am J Respir Cell Mol Biol* 2011;44: 276–284.
29. Bonser LR, Erle DJ. Putting mucins on the map. *Am J Respir Crit Care Med* 2019;199:681–682.
30. Bandura DR, Baranov VI, Ornatsky OI, Antonov A, Kinach R, Lou X, *et al*. Mass cytometry: technique for real time single cell multitarget immunoassay based on inductively coupled plasma time-of-flight mass spectrometry. *Anal Chem* 2009;81:6813–6822.
31. Akkaya B, Miozzo P, Holstein AH, Shevach EM, Pierce SK, Akkaya M. A simple, versatile antibody-based barcoding method for flow cytometry. *J Immunol* 2016;197:2027–2038.
32. Piperno G, Fuller MT. Monoclonal antibodies specific for an acetylated form of alpha-tubulin recognize the antigen in cilia and flagella from a variety of organisms. *J Cell Biol* 1985;101:2085–2094.
33. Basnet S, Bochkov YA, Brockman-Schneider RA, Kuipers I, Aesif SW, Jackson DJ, *et al*. *CDHR3* asthma-risk genotype affects susceptibility of airway epithelium to rhinovirus C infections. *Am J Respir Cell Mol Biol* 2019;61:450–458.
34. Bønnelykke K, Sleiman P, Nielsen K, Kreiner-Møller E, Mercader JM, Belgrave D, *et al*. A genome-wide association study identifies CDHR3 as a susceptibility locus for early childhood asthma with severe exacerbations. *Nat Genet* 2014;46:51–55.
35. Beane J, Sebastiani P, Liu G, Brody JS, Lenburg ME, Spira A. Reversible and permanent effects of tobacco smoke exposure on airway epithelial gene expression. *Genome Biol* 2007;8:R201.
36. Ooi AT, Gower AC, Zhang KX, Vick JL, Hong L, Nagao B, *et al*. Molecular profiling of premalignant lesions in lung squamous cell carcinomas identifies mechanisms involved in stepwise carcinogenesis. *Cancer Prev Res (Phila)* 2014;7:487–495.
37. Shikotra A, Choy DF, Siddiqui S, Arthur G, Nagarkar DR, Jia G, *et al*. A CEACAM6-high airway neutrophil phenotype and CEACAM6-high epithelial cells are features of severe asthma. *J Immunol* 2017;198: 3307–3317.